

Jensen-Shannon Divergence Based Loss Functions for Bayesian Neural Networks

Ponkrshnan Thiagarajan ^{a,1}, Susanta Ghosh ^{b,2}

^a*Department of Mechanical Engineering-Engineering Mechanics, Michigan Technological University, MI, USA*

^b*Mechanical Engineering-Engineering Mechanics and the Institute of Computing and Cybersystems, Michigan Technological University, MI, USA.*

Abstract

The Kullback-Leibler (KL) divergence is widely used for the variational inference of Bayesian Neural Networks (BNNs) to approximate the posterior distribution of weights. However, the KL divergence is unbounded and asymmetric, which may lead to instabilities during optimization or may yield poor generalizations. To overcome these limitations, we examine the Jensen-Shannon (JS) divergence that is more general, bounded, and symmetric. Towards this, we propose two novel loss functions for BNNs: 1) a geometric JS divergence (JS-G) based loss function that is symmetric but unbounded with closed-form expression for Gaussian priors and 2) a generalized JS divergence (JS-A) based loss function that is symmetric and bounded. We show that the conventional KL divergence-based loss function is a special case of the loss functions presented in this work. To evaluate the divergence part of the proposed JS-G-based loss function, we use an exact closed-form expression for Gaussian priors. For any other priors of JS-G and for the JS-A-based loss function we use Monte Carlo approximation. We provide algorithms to optimize the loss function using both these methods. The proposed loss functions offer additional parameters that can be tuned to control the regularisation. We explain the reason why the proposed loss functions should perform better than the state-of-the-art. Further, we derive the conditions under which the proposed JS-G-loss function regularises better than the KL divergence-based loss function for Gaussian priors and posteriors. The proposed JS divergence-based Bayesian convolutional neural networks (BCNN) perform better than the state-of-the-art BCNN, which is shown for the classification of the CIFAR data set having various degrees of noise and a biased histopathology data set.

Keywords: Bayesian convolutional neural networks, Variational inference, KL divergence, JS divergence, Uncertainty quantification.

1. Introduction

Despite the widespread success of deep neural networks (DNNs) and convolutional neural networks (CNNs) in numerous science and engineering applications [1–10], they suffer from overfitting when the data set is small, noisy or biased [3, 11]. Further, due to a very large number of (deterministic) parameters, CNNs cannot provide a robust measure of uncertainty. Without a measure of uncertainty in the predictions, erroneous predictions by these models may lead to catastrophic failures in applications that require high accuracies such as autonomous driving and medical diagnosis. Several methods were developed to provide prediction intervals as a measure of uncertainty in neural networks. Some of these include the delta method, bootstrap method, mean-variance estimation method, Bayesian method, etc. [12]. Amongst these, Bayesian methods have gained eminence due to their rigorous mathematical foundation for uncertainty quantification through their stochastic parameters [12, 13]. In the following, key aspects of Bayesian Neural Networks (BNNs) are briefly summarised.

¹email: thiagara@mtu.edu

²email: susantag@mtu.edu

This paper is to be submitted in IEEE for peer review.

We acknowledge Superior, a high-performance computing facility at MTU. This work used the XSEDE Bridges at the Pittsburgh Supercomputing Center through allocation No. MSS200004.

Bayesian Neural Networks (BNNs): A BNN is a neural network with stochastic parameters. The posterior distribution of these parameters is learned through the Bayes rule. The first known BNN developed by Tishby et al [14] showed that the posterior distributions of weights and biases can be obtained via the Bayes rule from a chosen prior. Though their work provided theoretical insights, a method to perform inference on the posterior distribution of parameters was still not available. To perform inference a Laplace approximation was proposed by Denker and LeCun [15]. Detailed reviews on BNNs are provided in [16, 17]. The two most commonly used techniques to approximate the posterior distribution of parameters (i.e. Bayesian inference) of a BNN are the Variational Inference (VI) and the Markov Chain Monte Carlo Methods (MCMC). MCMC methods comprise a set of algorithms to sample from arbitrary and intractable probability distributions. Inference of posterior using MCMC algorithms can be very accurate but they are computationally demanding [18]. In addition, MCMC algorithms do not scale well with the model size. Therefore, the VI-based approaches are focused on this work. A brief review of some of the early works VI techniques are presented in the following.

Variational Inference (VI) in Bayesian Neural Networks: VI is a technique to approximate an intractable posterior distribution by a tractable distribution called the variational distribution. The variational distribution is learned by minimizing its dissimilarity with respect to the true posterior. The first work that resembles VI was proposed by Hinton and Van Camp [19] to learn the posterior distribution of neural network parameters using an information theory-based approach. Their work factorized the posterior distribution of neural network parameters thereby neglecting the correlations between them. A full correlation between the network parameters was introduced by Barber and Bishop [20]. These two methods ([19, 20]) are focused on analytical representations of the optimization objective. Therefore they are limited to single hidden layer networks and could not be used for larger networks.

Recent Advances on Bayesian Neural Networks: High computational cost was the bottleneck for BNNs in the late 90s. With the advancement in GPU computation, research in the field of BNN has resurged. A data sub-sampling technique to scale for large amounts of data in a VI objective has been proposed by Graves [21]. In addition, their method minimized the evidence lower bound (ELBO) to learn the network parameters. While their method enabled the application of VI for large networks, it performs poorly due to high variance in the computed gradients via Monte Carlo approximation and also due to a lack of correlations between weights. To improve upon their approach a novel algorithm for backpropagation has been proposed by Hernandez et al [22]. Blundell et al. [23] reparametrized the stochastic variables and obtained unbiased gradient estimates of the loss function to facilitate backpropagation.

To summarise, VI methods are efficient and they scale well for larger networks and are thus widely used. Most of the VI technique in the literature uses the KL divergence as a measure of dissimilarity between the true and the variational posterior. However, the KL divergence has two key limitations, first, it is asymmetric with respect to its arguments, and second, its values are unbounded. These limitations may lead to poor generalization or failure during training as reported in [24]. Therefore, it is imperative to explore alternative divergences for VI that can alleviate these limitations.

In this regard, Renyi’s α -divergences have been introduced for VI by Li and Turner [25]. They proposed a family of variational methods that unified various existing approaches. A χ -divergence-based VI has been proposed by Dieng et al. [26] that provides an upper bound of the model evidence. Additionally, their results have shown better estimates for the variance of the posterior. Along these lines, an f-Divergence based VI has been proposed by Wan et al. to generalize VI for all f-divergences that unified the Reyni divergence [25] and χ divergence [26] based VIs. A modification to the skew-geometric Jensen-Shannon (JS) divergence has been proposed by Deasy et al. to introduce a new loss function for Variational Auto Encoders (VAEs) [27] which has shown a better reconstruction and generation as compared to existing VAEs. However, a JS divergence-based loss function is not yet available for BNNs.

Proposed Jensen-Shannon (JS) Divergence-based Loss Functions for Bayesian Neural Networks: In this work, we present a constrained optimization problem that results in two novel loss functions for BNNs namely the skew-geometric JS divergence-based loss function and a modified generalized JS divergence-based loss function. These loss functions are a generalization to the ELBO loss [21–23] obtained by VI of the posterior using KL divergence. We explain why these loss functions should perform better. In addition, we derive the conditions under which the proposed skew-geometric JS divergence-based loss function regularises better than the KL divergence-based loss function for Gaussian priors and posteriors. Further, we show that the loss functions presented in this work perform better on classification problems where the dataset is noisy or is biased towards a particular class.

The rest of the manuscript is organized as follows: Sec. 2 describes the proposed loss functions. The details of the numerical experiments are provided in Sec. 3. The results obtained by the present method are presented and discussed

in Sec. 4. Finally, conclusions are provided in Sec. 5.

2. Methods

2.1. Background: KL and JS divergences

Consider two random variables \mathcal{P} and \mathcal{Q} defined on a probability space Ω . The KL divergence between \mathcal{P} and \mathcal{Q} is defined as

$$\text{KL}[\mathcal{P} \parallel \mathcal{Q}] = \int_{\Omega} p(x) \log \left[\frac{p(x)}{q(x)} \right] dx \quad (1)$$

where $p(x)$ and $q(x)$ are the probability densities of \mathcal{P} and \mathcal{Q} respectively. For two n -dimensional multivariate Gaussian distributions³ $\mathcal{N}_1(\boldsymbol{\mu}_1, \boldsymbol{\Sigma}_1)$ and $\mathcal{N}_2(\boldsymbol{\mu}_2, \boldsymbol{\Sigma}_2)$, the KL divergence is given by

$$\text{KL}(\mathcal{N}_1 \parallel \mathcal{N}_2) = \frac{1}{2} \left[\text{tr}(\boldsymbol{\Sigma}_2^{-1} \boldsymbol{\Sigma}_1) + \ln \frac{|\boldsymbol{\Sigma}_2|}{|\boldsymbol{\Sigma}_1|} + (\boldsymbol{\mu}_2 - \boldsymbol{\mu}_1)^T \boldsymbol{\Sigma}_2^{-1} (\boldsymbol{\mu}_2 - \boldsymbol{\mu}_1) - n \right] \quad (2)$$

The KL divergence is widely used in literature to represent the dissimilarity between two probability distributions for various applications such as VI. However, it has limitations such as the asymmetric property i.e $\text{KL}[\mathcal{P} \parallel \mathcal{Q}] \neq \text{KL}[\mathcal{Q} \parallel \mathcal{P}]$, and unboundedness. These limitations may lead to difficulty in approximating light-tailed posteriors as reported in [24].

To overcome these limitations a symmetric JS divergence can be employed. JS divergence is defined as

$$\text{JS}[\mathcal{P} \parallel \mathcal{Q}] = \frac{1}{2} \text{KL} \left[p \parallel \frac{p+q}{2} \right] + \frac{1}{2} \text{KL} \left[q \parallel \frac{p+q}{2} \right] \quad (3)$$

More generally, with the weighted arithmetic mean of p and q defined as $A_{\alpha} = (1 - \alpha)p + \alpha q$,

$$\text{JS}^{A_{\alpha}}[\mathcal{P} \parallel \mathcal{Q}] = (1 - \alpha) \text{KL}(p \parallel A_{\alpha}) + \alpha \text{KL}(q \parallel A_{\alpha}) \quad (4)$$

Although this JS divergence is symmetric and bounded, unlike the KL divergence its analytical expression cannot be obtained even when p and q are Gaussians. To overcome this difficulty a generalization of the JS divergence using abstract means, specifically the geometric mean was proposed by Nielsen [28]. By considering the weighted geometric mean $G_{\alpha}(x, y) = x^{1-\alpha}y^{\alpha}$ for two real variables x and y , where $\alpha \in [0, 1]$, the following new family of skew geometric divergence has been introduced in [28],

$$\text{JS}^{G_{\alpha}}[\mathcal{P} \parallel \mathcal{Q}] = (1 - \alpha) \text{KL}(p \parallel G_{\alpha}(p, q)) + \alpha \text{KL}(q \parallel G_{\alpha}(p, q)) \quad (5)$$

The parameter α , called a skew parameter, controls the divergence skew between p and q . However, the skew-geometric divergence in Eq.(5) fails to capture the divergence between p and q in the limits of α since it yields zeros. To resolve this issue, Deasy et al. [27] used the following reverse form of geometric mean $G'_{\alpha}(x, y) = x^{\alpha}y^{1-\alpha}$, with $\alpha \in [0, 1]$ to implement JS divergence in variational autoencoders. The JS divergence with this reverse of the geometric mean is given by

$$\text{JS-G}[\mathcal{P} \parallel \mathcal{Q}] = (1 - \alpha) \text{KL}(p \parallel G'_{\alpha}(p, q)) + \alpha \text{KL}(q \parallel G'_{\alpha}(p, q)) \quad (6)$$

This yields KL divergences in the limiting values of the skew parameter.

In the case of two multivariate Gaussian distributions, the JS-G can be written as

$$\begin{aligned} \text{JS-G}(\mathcal{N}_1 \parallel \mathcal{N}_2) &= (1 - \alpha) \text{KL}(\mathcal{N}_1 \parallel \mathcal{N}'_{\alpha}) + \alpha \text{KL}(\mathcal{N}_2 \parallel \mathcal{N}'_{\alpha}) \\ &= \frac{1}{2} \left[\text{tr} \left(\frac{(1 - \alpha) \boldsymbol{\Sigma}_1 + \alpha \boldsymbol{\Sigma}_2}{\boldsymbol{\Sigma}'_{\alpha}} \right) + \log \left(\frac{|\boldsymbol{\Sigma}'_{\alpha}|}{|\boldsymbol{\Sigma}_1|^{1-\alpha} |\boldsymbol{\Sigma}_2|^{\alpha}} \right) + (1 - \alpha) (\boldsymbol{\mu}'_{\alpha} - \boldsymbol{\mu}_1)^T \boldsymbol{\Sigma}_{\alpha}^{-1} (\boldsymbol{\mu}'_{\alpha} - \boldsymbol{\mu}_1) + \alpha (\boldsymbol{\mu}'_{\alpha} - \boldsymbol{\mu}_2)^T \boldsymbol{\Sigma}_{\alpha}^{-1} (\boldsymbol{\mu}'_{\alpha} - \boldsymbol{\mu}_2) - n \right] \end{aligned} \quad (7)$$

³ \mathcal{N} denotes a Gaussian distribution throughout this work.

where, $\mathcal{N}'_\alpha \sim \mathcal{N}(\mu'_\alpha, \Sigma'_\alpha)$ is an intermediate mean distribution with the parameters

$$\Sigma'_\alpha = [\alpha \Sigma_1^{-1} + (1 - \alpha) \Sigma_2^{-1}]^{-1} \quad (8)$$

$$\mu'_\alpha = \Sigma_\alpha [\alpha \Sigma_1^{-1} \mu_1 + (1 - \alpha) \Sigma_2^{-1} \mu_2] \quad (9)$$

Proposition 1. (Symmetry)

For $\alpha \in [0, 1]$, $JS-G(N_1||N_2)|_\alpha = JS-G(N_2||N_1)|_{1-\alpha}$. This implies for the special case of $\alpha = 0.5$, $JS-G(N_1||N_2)|_{\alpha=0.5} = JS-G(N_2||N_1)|_{\alpha=0.5}$.

It is important to note that although the geometric JS divergences given in Eq.(5) and Eq.(6) have an analytical expression when p and q are Gaussians, they lose their upper bound property. In other words, they are unbounded like the KL divergence as shown in Table 1. Whereas, the generalized JS divergence is both bounded and symmetric.

We propose two novel loss functions for BNNs: 1) based on a modification to the generalized JS divergence given in Eq.(4) and implement it using MC sampling due to the lack of closed form 2) based on the skew-geometric JS divergence in Eq.(6) and implement it using analytical expression.

Table 1: Properties of divergences

Divergence	Bounded	Symmetric	Analytical expression
KL	×	×	✓
JS^{A_α}	✓	✓	×
JS-G	×	✓	✓

2.2. Background: Variational inference

Given a set of training data $\mathbb{D} = \{\mathbf{x}_i, \mathbf{y}_i\}_{i=1}^N$ and test input, $\mathbf{x} \in \mathbb{R}^p$, we are interested in learning a data-driven model (for instance a BNN) to predict the probability $P(\mathbf{y}|\mathbf{x}, \mathbb{D})$ of output $\mathbf{y} \in \Upsilon$, where Υ is the output space. To this end we train a neural network with random parameters \mathbf{w} and learn the posterior probability distribution of these parameters $P(\mathbf{w}|\mathbb{D})$ from the training data \mathbb{D} using the Bayes' rule as follows:

$$P(\mathbf{w}|\mathbb{D}) = \frac{P(\mathbb{D}|\mathbf{w})P(\mathbf{w})}{P(\mathbb{D})} \quad (10)$$

Where, $P(\mathbb{D}|\mathbf{w})$ is the likelihood of the training data \mathbb{D} given parameters \mathbf{w} . $P(\mathbf{w})$ is the prior distribution of weights. The term $P(\mathbb{D})$, called the evidence, involves marginalization over the distribution of weights: $P(\mathbb{D}) = \int_{\Omega_w} P(\mathbb{D}|\mathbf{w})P(\mathbf{w})d\mathbf{w}$

Using the posterior distribution of weights, the predictive distribution of the output can be obtained by marginalizing the weights as

$$P(\mathbf{y}|\mathbf{x}, \mathbb{D}) = \int_{\Omega_w} P(\mathbf{y}|\mathbf{x}, \mathbf{w})P(\mathbf{w}|\mathbb{D})d\mathbf{w} \quad (11)$$

The term $P(\mathbb{D})$ in Eq. (10) is intractable due to marginalization over \mathbf{w} , which in turn makes $P(\mathbf{w}|\mathbb{D})$ intractable. To alleviate this difficulty, the posterior is approximated using variational inference.

In variational inference, the unknown intractable posterior $P(\mathbb{D}|\mathbf{w})$ is approximated by a known simpler distribution $q(\mathbf{w}|\theta)$ over the model weights. $q(\mathbf{w}|\theta)$ is referred to as the variational posterior having parameters θ . For example, if q is assumed to be a Gaussian distribution then the parameters θ are the mean μ and the standard deviation σ . In variational inference, the set of parameters θ for the model weights are learned by minimizing the divergence (e.g. KL divergence) between $P(\mathbf{w}|\mathbb{D})$ and $q(\mathbf{w}|\theta)$ as shown in [23].

$$\begin{aligned} \theta^* &= \arg \min_{\theta} \text{KL} [q(\mathbf{w}|\theta) || P(\mathbf{w}|\mathbb{D})] \\ &= \arg \min_{\theta} \int q(\mathbf{w}|\theta) \log \left[\frac{q(\mathbf{w}|\theta)}{P(\mathbf{w})P(\mathbb{D}|\mathbf{w})} P(\mathbb{D}) \right] d\mathbf{w} \end{aligned} \quad (12)$$

Note that the term $P(\mathbb{D})$ can be eliminated from Eq. (12) since it is a constant and does not affect the optimization. The resulting loss function $\mathcal{F}(\mathbb{D}, \theta)$, which is to be minimised to learn the optimal parameters θ^* is expressed as:

$$\mathcal{F}(\mathbb{D}, \theta) = \text{KL}[q(\mathbf{w}|\theta) \| P(\mathbf{w})] - \mathbb{E}_{q(\mathbf{w}|\theta)}[\log P(\mathbb{D}|\mathbf{w})] \quad (13)$$

This loss function is known as the variational free energy or the evidence lower bound.

2.3. Proposed modification to the generalized JS divergence

The Generalised JS divergence given in Eq. (4) fails to capture the divergence between p and q in the limiting cases of α .

$$\left[\text{JS}^{A_\alpha}(\mathcal{P} \| \mathcal{Q}) \right]_{\alpha=0} = 0 \quad \left[\text{JS}^{A_\alpha}(\mathcal{P} \| \mathcal{Q}) \right]_{\alpha=1} = 0 \quad (14)$$

To overcome this difficulty we propose to modify the weighted arithmetic mean as $A'_\alpha = \alpha p + (1 - \alpha)q$ yielding the following modification to the generalized JS divergence.

$$\text{JS-A}[\mathcal{P} \| \mathcal{Q}] = (1 - \alpha)\text{KL}(p \| A'_\alpha) + \alpha\text{KL}(q \| A'_\alpha) \quad (15)$$

This modification yields KL divergences in the limiting cases as

$$[\text{JS-A}(\mathcal{P} \| \mathcal{Q})]_{\alpha=0} = \text{KL}(\mathcal{P} \| \mathcal{Q}) \quad [\text{JS-A}(\mathcal{P} \| \mathcal{Q})]_{\alpha=1} = \text{KL}(\mathcal{Q} \| \mathcal{P}) \quad (16)$$

Theorem 1: (Boundedness)

For any two distributions $P_1(t)$ and $P_2(t)$, $t \in \Omega$, the value of the divergence JS-A is bounded such that,

$$\text{JS-A} \leq -(1 - \alpha) \log \alpha - \alpha \log(1 - \alpha)$$

Proof:

$$\begin{aligned} \text{JS-A} &= (1 - \alpha) \int_{\Omega} P_1 \log \frac{P_1}{A'_\alpha} dt + \alpha \int_{\Omega} P_2 \log \frac{P_2}{A'_\alpha} dt \\ &= \int_{\Omega} A'_\alpha \left[(1 - \alpha) \frac{P_1}{A'_\alpha} \log \frac{P_1}{A'_\alpha} + \alpha \frac{P_2}{A'_\alpha} \log \frac{P_2}{A'_\alpha} \right] dt \\ &= \int_{\Omega} A'_\alpha \left[\frac{(1 - \alpha) \alpha P_1}{\alpha} \left(\log \frac{\alpha P_1}{A'_\alpha} - \log \alpha \right) + \frac{\alpha}{(1 - \alpha)} \frac{(1 - \alpha) P_2}{A'_\alpha} \left(\log \frac{(1 - \alpha) P_2}{A'_\alpha} - \log(1 - \alpha) \right) \right] dt \\ &= \int_{\Omega} -(1 - \alpha) P_1 \log \alpha dt - \int_{\Omega} \alpha P_2 \log(1 - \alpha) dt - \frac{(1 - \alpha)}{\alpha} H\left(\frac{\alpha P_1}{A'_\alpha}\right) - \frac{\alpha}{(1 - \alpha)} H\left(\frac{(1 - \alpha) P_2}{A'_\alpha}\right) \\ &= -(1 - \alpha) \log \alpha - \alpha \log(1 - \alpha) - \frac{(1 - \alpha)}{\alpha} H\left(\frac{\alpha P_1}{A'_\alpha}\right) - \frac{\alpha}{(1 - \alpha)} H\left(\frac{(1 - \alpha) P_2}{A'_\alpha}\right) \\ &\leq -(1 - \alpha) \log \alpha - \alpha \log(1 - \alpha) \end{aligned}$$

Where, $H(f(t)) = - \int_{\Omega} f(t) \log f(t) dt$. Further, $H(f(t)) \geq 0$; $\forall f(t) \in [0, 1]$

2.4. Proposed JS divergence-based loss function

2.4.1. Intractability of the JS-based variational inference

We propose to use the more general JS divergence as a measure of dissimilarity between the true posterior $P(\mathbf{w}|\mathbb{D})$ and the variational posterior $q(\mathbf{w}|\theta)$ in Eq. (12). Therefore, the optimization problem becomes,

$$\theta^* = \arg \min_{\theta} \text{JS-G}[q(\mathbf{w}|\theta) \| P(\mathbf{w}|\mathbb{D})] \quad (17)$$

The loss function can then be written as,

$$\begin{aligned} \hat{\mathcal{F}}(\mathbb{D}, \theta) &= \text{JS-G}[q(\mathbf{w}|\theta) \| P(\mathbf{w}|\mathbb{D})] \\ &= (1 - \alpha)\text{KL}(q \| G'_\alpha(q, P)) + \alpha\text{KL}(P \| G'_\alpha(q, P)) \end{aligned} \quad (18)$$

Where, $G'_\alpha(q, P) = q(\mathbf{w}|\boldsymbol{\theta})^\alpha P(\mathbf{w}|\mathbb{D})^{(1-\alpha)}$.
Rewriting the first term in Eq. (18) as,

$$\begin{aligned} T_1 &= (1 - \alpha) \text{KL}(q \| G'_\alpha(q, P)) \\ &= (1 - \alpha) \text{KL}[q(\mathbf{w}|\boldsymbol{\theta}) \| q(\mathbf{w}|\boldsymbol{\theta})^\alpha P(\mathbf{w}|\mathbb{D})^{(1-\alpha)}] \\ &= (1 - \alpha) \int q(\mathbf{w}|\boldsymbol{\theta}) \log \left[\frac{q(\mathbf{w}|\boldsymbol{\theta})}{q(\mathbf{w}|\boldsymbol{\theta})^\alpha P(\mathbf{w}|\mathbb{D})^{1-\alpha}} \right] d\mathbf{w} \\ &= (1 - \alpha)^2 \int q(\mathbf{w}|\boldsymbol{\theta}) \log \left[\frac{q(\mathbf{w}|\boldsymbol{\theta})}{P(\mathbf{w}|\mathbb{D})} \right] d\mathbf{w} \end{aligned} \quad (19)$$

which is equivalent to loss function in Eq. (13) multiplied by a constant $(1 - \alpha)^2$. Similarly rewriting the second term in Eq. (18) as,

$$\begin{aligned} T_2 &= \alpha \text{KL}(P \| G'_\alpha(q, P)) \\ &= \alpha \text{KL}[P(\mathbf{w}|\mathbb{D}) \| q(\mathbf{w}|\boldsymbol{\theta})^\alpha P(\mathbf{w}|\mathbb{D})^{(1-\alpha)}] \\ &= \alpha \int P(\mathbf{w}|\mathbb{D}) \log \left[\frac{P(\mathbf{w}|\mathbb{D})}{q(\mathbf{w}|\boldsymbol{\theta})^\alpha P(\mathbf{w}|\mathbb{D})^{(1-\alpha)}} \right] d\mathbf{w} \\ &= \alpha^2 \int P(\mathbf{w}|\mathbb{D}) \log \left[\frac{P(\mathbf{w}|\mathbb{D})}{q(\mathbf{w}|\boldsymbol{\theta})} \right] d\mathbf{w} \end{aligned} \quad (20)$$

The term $P(\mathbf{w}|\mathbb{D})$ in Eq. (20) is intractable following the explanation in section 2.2, which makes T_2 intractable.⁴ Therefore the JS divergence-based loss function given in Eq. (18) cannot be used to find the optimum parameter $\boldsymbol{\theta}^*$ which contrasts the KL divergence based loss function in Eq. (13). This result can be shown for the JS-A divergence following similar steps.

To overcome this challenge, we propose to derive a loss function for BNNs in a constrained optimization framework. We show that such a loss function is equivalent to the loss function obtained through variational inference.

2.4.2. Loss function derived using a constrained optimisation framework

We propose a novel JS divergence-based loss function for BNNs following the constrained optimization framework for variational autoencoders [27, 29]. Given a set of training data \mathbb{D} , we are interested in learning the probability distribution $q(\mathbf{w}|\boldsymbol{\theta})$ of parameters of the neural network such that, the likelihood of observing the data given the parameters are maximized. Thus, the optimization problem can be written as

$$\max_{\boldsymbol{\theta}} \mathbb{E}_{q(\mathbf{w}|\boldsymbol{\theta})} [\log P(\mathbb{D}|\mathbf{w})] \quad (21)$$

Where $\boldsymbol{\theta}$ is a set of parameters of the inferred probability distribution $q(\mathbf{w}|\boldsymbol{\theta})$. This optimization is constrained to make $q(\mathbf{w}|\boldsymbol{\theta})$ similar to a prior $P(\mathbf{w})$. This leads to a constrained optimization problem as given below:

$$\max_{\boldsymbol{\theta}} \mathbb{E}_{q(\mathbf{w}|\boldsymbol{\theta})} [\log P(\mathbb{D}|\mathbf{w})] \quad \text{subject to } D(q(\mathbf{w}|\boldsymbol{\theta}) \| P(\mathbf{w})) < \epsilon \quad (22)$$

where ϵ determines the strength of the applied constraint and D is a divergence measure. Following the KKT approach, the Lagrangian function corresponding to the constrained optimization problem can be written as

$$\mathcal{L} = \mathbb{E}_{q(\mathbf{w}|\boldsymbol{\theta})} [\log P(\mathbb{D}|\mathbf{w})] - \lambda(D(q(\mathbf{w}|\boldsymbol{\theta}) \| P(\mathbf{w})) - \epsilon) \quad (23)$$

Here ϵ is a constant which can be removed from the optimization. Also changing the sign of the above equations leads to the following loss function that needs to be minimized.

$$\tilde{\mathcal{F}} = \lambda D(q(\mathbf{w}|\boldsymbol{\theta}) \| P(\mathbf{w})) - \mathbb{E}_{q(\mathbf{w}|\boldsymbol{\theta})} [\log P(\mathbb{D}|\mathbf{w})] \quad (24)$$

This loss function yields ELBO loss [23] when KL divergence is considered as the divergence measure D and λ is taken as 1.

⁴We obtain a similar result when the geometric mean G_α is used. Only the constants outside the integral change in that case.

2.4.3. Geometric J-S divergence

We propose to use the modified skew-geometric JS divergence as the divergence measure, D , in Eq.(24) which leads to the following loss function:

$$\begin{aligned}\widetilde{\mathcal{F}}_{JSG} &= \lambda \text{JS-G}(q(\mathbf{w}|\boldsymbol{\theta}) \parallel P(\mathbf{w})) - \mathbb{E}_{q(\mathbf{w}|\boldsymbol{\theta})} [\log P(\mathbb{D}|\mathbf{w})] \\ &= \lambda(1 - \alpha) \text{KL}(q \parallel G'_\alpha(q, P_w)) + \lambda\alpha \text{KL}(P_w \parallel G'_\alpha(q, P_w)) - \mathbb{E}_{q(\mathbf{w}|\boldsymbol{\theta})} [\log P(\mathbb{D}|\mathbf{w})]\end{aligned}\quad (25)$$

Note,

$$\begin{aligned}\text{KL}(q \parallel G'_\alpha(q, P_w)) &= \int q(\mathbf{w}|\boldsymbol{\theta}) \log \frac{q(\mathbf{w}|\boldsymbol{\theta})}{q(\mathbf{w}|\boldsymbol{\theta})^\alpha P(\mathbf{w})^{1-\alpha}} d\mathbf{w} \\ &= (1 - \alpha) \int q(\mathbf{w}|\boldsymbol{\theta}) \log \frac{q(\mathbf{w}|\boldsymbol{\theta})}{P(\mathbf{w})} d\mathbf{w}\end{aligned}\quad (26)$$

and

$$\begin{aligned}\text{KL}(P_w \parallel G'_\alpha(q, P_w)) &= \int P(\mathbf{w}) \log \frac{P(\mathbf{w})}{q(\mathbf{w}|\boldsymbol{\theta})^\alpha P(\mathbf{w})^{1-\alpha}} d\mathbf{w} \\ &= \alpha \int P(\mathbf{w}) \log \frac{P(\mathbf{w})}{q(\mathbf{w}|\boldsymbol{\theta})} d\mathbf{w}\end{aligned}\quad (27)$$

Hence, the loss function can be written as,

$$\widetilde{\mathcal{F}}_{JSG} = \lambda(1 - \alpha)^2 \int q(\mathbf{w}|\boldsymbol{\theta}) \log \frac{q(\mathbf{w}|\boldsymbol{\theta})}{P(\mathbf{w})} d\mathbf{w} + \lambda\alpha^2 \int P(\mathbf{w}) \log \frac{P(\mathbf{w})}{q(\mathbf{w}|\boldsymbol{\theta})} d\mathbf{w} - \mathbb{E}_{q(\mathbf{w}|\boldsymbol{\theta})} [\log P(\mathbb{D}|\mathbf{w})] \quad (28)$$

Eq. (28) can be rewritten in terms of expectations as,

$$\widetilde{\mathcal{F}}_{JSG} = \lambda(1 - \alpha)^2 \mathbb{E}_{q(\mathbf{w}|\boldsymbol{\theta})} \left[\log \frac{q(\mathbf{w}|\boldsymbol{\theta})}{P(\mathbf{w})} \right] + \lambda\alpha^2 \mathbb{E}_{P(\mathbf{w})} \left[\log \frac{P(\mathbf{w})}{q(\mathbf{w}|\boldsymbol{\theta})} \right] - \mathbb{E}_{q(\mathbf{w}|\boldsymbol{\theta})} [\log P(\mathbb{D}|\mathbf{w})] \quad (29)$$

In Eq.(28), the first term is the *mode seeking* reverse KL divergence $\text{KL}(q(\mathbf{w}|\boldsymbol{\theta}) \parallel P(\mathbf{w}))$ and the second term is the *mean seeking* forward KL divergence $\text{KL}(P(\mathbf{w}) \parallel q(\mathbf{w}|\boldsymbol{\theta}))$. Therefore, the proposed loss function offers a weighted sum of the forward and reverse KL divergences in contrast to only the reverse KL divergence in ELBO. Whereas the likelihood part remains identical. This should ensure better regularisation by imposing stricter penalization if the posterior is away from the prior distribution which will be demonstrated in Sec. 2.7.1. The parameters λ and α can be used to control the amount of regularisation.

2.4.4. Modified Generalised J-S divergence

Using the modified Generalised JS divergence as the divergence measure, D in Eq.(24) leads to the following loss function:

$$\begin{aligned}\widetilde{\mathcal{F}}_{JSA} &= \lambda \text{JS-A}(q(\mathbf{w}|\boldsymbol{\theta}) \parallel P(\mathbf{w})) - \mathbb{E}_{q(\mathbf{w}|\boldsymbol{\theta})} [\log P(\mathbb{D}|\mathbf{w})] \\ &= \lambda(1 - \alpha) \text{KL}(q \parallel A'_\alpha(q, P_w)) + \lambda\alpha \text{KL}(P_w \parallel A'_\alpha(q, P_w)) - \mathbb{E}_{q(\mathbf{w}|\boldsymbol{\theta})} [\log P(\mathbb{D}|\mathbf{w})]\end{aligned}\quad (30)$$

Where, $A'_\alpha(q, P_w) = \alpha q + (1 - \alpha)P_w$. Since the divergence part of the loss function in Eq. (30) cannot be evaluated with analytical expressions, we resort to Monte Carlo sampling as shown in Algorithm 2.

It is to be noted that the proposed loss functions in Eq. (25) and Eq. (30) yield the ELBO loss for $\alpha = 0$ and $\lambda = 1$.

2.5. Minimisation of the loss function: evaluation of the divergence in a closed-form

In this subsection, we describe the minimization of the loss function by evaluating the divergence in closed-form for Gaussian priors. The closed-form expression of the JS divergence for Gaussian priors is presented in Sec.2.4.2. Assuming the prior and the likelihood are Gaussians, the posterior will also be a Gaussian. The Gaussian posterior is denoted by $q_N(\mathbf{w}) \sim \mathcal{N}(\boldsymbol{\mu}_1, \boldsymbol{\Sigma}_1^2)$ and the Gaussian prior is denoted as $P_N(\mathbf{w}|\boldsymbol{\theta}) \sim \mathcal{N}(\boldsymbol{\mu}_2, \boldsymbol{\Sigma}_2^2)$, where the subscript

$()_N$ indicates Gaussian distribution. $\boldsymbol{\mu}_1$ and $\boldsymbol{\mu}_2$ are n -dimensional vectors and $\boldsymbol{\Sigma}_1^2, \boldsymbol{\Sigma}_2^2$ are assumed to be diagonal matrices such that $\boldsymbol{\mu}_1 = [\mu_{11}, \mu_{12}, \dots, \mu_{1n}]^T$ and $\boldsymbol{\Sigma}_1^2 = \text{diag}(\sigma_{11}^2, \sigma_{12}^2, \dots, \sigma_{1n}^2)$ (similarly for $\boldsymbol{\mu}_2$ and $\boldsymbol{\Sigma}_2^2$). The JS divergence (JS-G) can be written as,

$$\text{JS-G}(q_N \| P_N) = \frac{1}{2} \sum_{i=1}^n \left[\frac{(1-\alpha)\sigma_{1i}^2 + \alpha\sigma_{2i}^2}{\sigma_{ai}^2} + \log \frac{(\sigma'_{ai})^2}{\sigma_{1i}^{2(1-\alpha)} \sigma_{2i}^{2\alpha}} + (1-\alpha) \frac{(\mu'_{ai} - \mu_{1i})^2}{(\sigma'_{ai})^2} + \frac{\alpha(\mu'_{ai} - \mu_{2i})^2}{(\sigma'_{ai})^2} - 1 \right] \quad (31)$$

where,

$$(\sigma'_{ai})^2 = \frac{\sigma_{1i}^2 \sigma_{2i}^2}{(1-\alpha)\sigma_{1i}^2 + \alpha\sigma_{2i}^2} \quad \mu'_{ai} = (\sigma'_{ai})^2 \left[\frac{\alpha\mu_{1i}}{\sigma_{1i}^2} + \frac{(1-\alpha)\mu_{2i}}{\sigma_{2i}^2} \right] \quad (32)$$

Therefore, the divergence term of the proposed loss function (Eq. (25)) can be replaced by this closed form expression given in Eq. (31). The second term, which is the expectation of the log-likelihood ($\mathbb{E}_{q(\mathbf{w}|\boldsymbol{\theta})} [\log P(\mathbb{D}|\mathbf{w})]$) can be approximated by a Monte-Carlo sampling as shown in the algorithm 1. Where, $\boldsymbol{\theta} = (\boldsymbol{\mu}, \boldsymbol{\rho})$ are the parameters of

Algorithm 1 Closed form implementation.

Evaluate JS-G from Eq. (31)

Evaluate $\mathbb{E}_{q(\mathbf{w}|\boldsymbol{\theta})} [\log P(\mathbb{D}|\mathbf{w})]$

Sample $\boldsymbol{\varepsilon}_i \sim \mathcal{N}(0, 1); i = 1, \dots, \text{No. of samples}$

$\mathbf{w}_i \leftarrow \boldsymbol{\mu} + \log(1 + \exp(\boldsymbol{\rho})) \circ \boldsymbol{\varepsilon}_i$.

$f_{ll} \leftarrow \sum_i \log P(\mathbb{D}|\mathbf{w}_i)$

Loss:

$$F \leftarrow \lambda \text{JS-G} - f_{ll}$$

Gradients:

$$\begin{aligned} \frac{\partial F}{\partial \boldsymbol{\mu}} &\leftarrow \sum_i \frac{\partial F}{\partial \mathbf{w}_i} + \frac{\partial F}{\partial \boldsymbol{\mu}} \\ \frac{\partial F}{\partial \boldsymbol{\rho}} &\leftarrow \sum_i \frac{\partial F}{\partial \mathbf{w}_i} \frac{\boldsymbol{\varepsilon}_i}{1 + \exp(-\boldsymbol{\rho})} + \frac{\partial F}{\partial \boldsymbol{\rho}} \end{aligned}$$

Update:

$$\begin{aligned} \boldsymbol{\mu} &\leftarrow \boldsymbol{\mu} - \beta \frac{\partial F}{\partial \boldsymbol{\mu}} \\ \boldsymbol{\rho} &\leftarrow \boldsymbol{\rho} - \beta \frac{\partial F}{\partial \boldsymbol{\rho}} \end{aligned}$$

the posterior distribution of weights that we wish to learn. Here, the reparametrization trick is used to separate the deterministic and the stochastic variables.

2.6. Minimization of the loss function: evaluation of the divergence via a Monte Carlo sampling

The algorithm provided in the previous subsection 2.5 (algorithm 1) is applicable to the JS-G divergence-based loss function, $\tilde{\mathcal{F}}_{JSG}$, only when the priors and the posterior distributions are assumed to be Gaussian. To provide a more general algorithm that removes this restriction for $\tilde{\mathcal{F}}_{JSG}$ and to evaluate the JS-A divergence-based loss function, $\tilde{\mathcal{F}}_{JSA}$, a Monte Carlo sampling technique can be used to minimize the loss function given in Eq. (29). The expectations in Eq. (29) can be approximated using Monte Carlo samples from the corresponding distributions as shown in the algorithm 2.

Algorithm 2 Monte Carlo implementation

Approximate $\mathbb{E}_{q(\mathbf{w}|\theta)}$

Sample $\boldsymbol{\varepsilon}_i^q \sim \mathcal{N}(0, 1); i = 1, \dots, \text{No. of samples}$

$$\mathbf{w}_i^q \leftarrow \boldsymbol{\mu} + \log(1 + \exp(\boldsymbol{\rho})) \circ \boldsymbol{\varepsilon}_i^q.$$

Evaluate JS-G:

$$f_1 \leftarrow \sum_i c_1 \log q(\mathbf{w}_i^q | \boldsymbol{\theta}) - c_1 \log P(\mathbf{w}_i^q) - \log P(\mathbb{D} | \mathbf{w}_i^q)$$

$$\text{where, } c_1 = \lambda(1 - \alpha)^2$$

(or)

Evaluate JS-A:

$$f_1 \leftarrow \sum_i c_1 \log q(\mathbf{w}_i^q | \boldsymbol{\theta}) - c_1 \log A_\alpha(\mathbf{w}_i^q) - \log P(\mathbb{D} | \mathbf{w}_i^q)$$

$$\text{where, } c_1 = \lambda(1 - \alpha)$$

Approximate $\mathbb{E}_{P(\mathbf{w})}$

Sample $\mathbf{w}_j^p \sim P(\mathbf{w}); j = 1, \dots, \text{No. of samples}$

Evaluate JS-G:

$$f_2 \leftarrow \sum_j c_2 \log P(\mathbf{w}_j^p) - c_2 \log q(\mathbf{w}_j^p | \boldsymbol{\theta})$$

$$\text{where, } c_2 = \lambda\alpha^2$$

(or)

Evaluate JS-A:

$$f_2 \leftarrow \sum_j c_2 \log A'_\alpha(\mathbf{w}_j^p) - c_2 \log q(\mathbf{w}_j^p | \boldsymbol{\theta})$$

$$\text{where, } c_2 = \lambda\alpha^2$$

Loss:

$$F \leftarrow f_1 + f_2$$

Gradients:

$$\frac{\partial F}{\partial \boldsymbol{\mu}} \leftarrow \sum_i \frac{\partial F}{\partial \mathbf{w}_i^q} + \frac{\partial F}{\partial \boldsymbol{\mu}}$$

$$\frac{\partial F}{\partial \boldsymbol{\rho}} \leftarrow \sum_i \frac{\partial F}{\partial \mathbf{w}_i^q} \frac{\boldsymbol{\varepsilon}_i}{1 + \exp(-\boldsymbol{\rho})} + \frac{\partial F}{\partial \boldsymbol{\rho}}$$

Update:

$$\boldsymbol{\mu} \leftarrow \boldsymbol{\mu} - \beta \frac{\partial F}{\partial \boldsymbol{\mu}}$$

$$\boldsymbol{\rho} \leftarrow \boldsymbol{\rho} - \beta \frac{\partial F}{\partial \boldsymbol{\rho}}$$

2.7. Insights into the advantages of JS divergence-based loss functions

To better understand the proposed JS divergence-based loss functions, we make use of contrived examples to compare them against the conventional KL divergence-based loss function. In the following we explore two aspects of the proposed loss functions:

1. The ability to regularize.

2. The advantage of using the closed-form expression over the Monte Carlo approximation while evaluating the JS-G divergence.

2.7.1. Regularisation performance of JS-G divergence

Let two Gaussian distributions $q \sim \mathcal{N}(\mu_1 = \mu, \sigma_1^2 = 0.01)$ and $P \sim \mathcal{N}(\mu_2 = 0, \sigma_2^2 = 0.1)$ mimic the posterior and the prior parameter of the BNN respectively. The closed-form divergences for KL and JS-G are evaluated by varying the q distribution's mean (μ). This is similar to learning the parameters of the network during training. The values of the divergences are plotted in Fig. 1. It is seen from Fig. 1 that, as the mean of the distribution q (i.e the

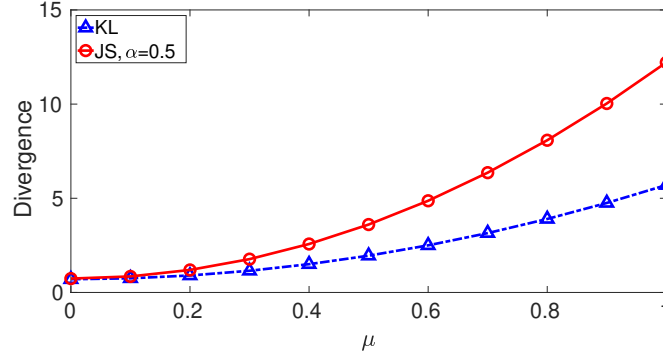


Figure 1: The value of divergence is plotted against the mean μ of q . Since the mean of P is fixed to zero, μ is also the difference in the mean values between the two distributions q and P

network parameter) diverges away from the mean of the distribution P (i.e the prior distribution) the value of the JS-G divergence is much more significant as compared to the KL divergence. This implies that the proposed JS-G divergence-based loss function is penalized higher than the KL divergence-based loss function if the mean of the network parameter is farther away from its prior distribution. Thus, by assuming small values for the means of prior distributions of the network parameters and finding the right value of α we can regularise the network parameters better in the case of the proposed JS -G divergence-based loss function.

2.7.2. Condition for better regularisation of $\tilde{\mathcal{F}}_{JS-G}$

The above example shows that the JS-G divergence is higher than KL for specific distributions $q \sim \mathcal{N}(\mu_1 = \mu, \sigma_1^2 = 0.01)$ and $P \sim \mathcal{N}(\mu_2 = 0, \sigma_2^2 = 0.1)$ and a given value of $\alpha = 0.5$. For any two arbitrary distributions, we propose the following theorems.

Theorem 2. For any two arbitrary distributions P and q , $\exists \alpha \in [0, \infty) : \tilde{\mathcal{F}}_{JS-G} > \mathcal{F}_{KL}$

Proof:

$$\tilde{\mathcal{F}}_{JS-G} - \mathcal{F}_{KL} > 0 \quad (33a)$$

$$(1 - \alpha)^2 \text{KL}(q||P) + \alpha^2 \text{KL}(P||q) - \text{KL}(q||P) > 0 \quad (33b)$$

$$(\alpha^2 - 2\alpha) \text{KL}(q||P) + \alpha^2 \text{KL}(P||q) > 0 \quad (33c)$$

$$\implies \alpha > \frac{2 \text{KL}(q||P)}{\text{KL}(q||P) + \text{KL}(P||q)} \quad (33d)$$

This is the condition on α for which JS divergence-based loss function regularises better than the KL divergence-based loss function. Further,

$$\frac{2 \text{KL}(q||P)}{\text{KL}(q||P) + \text{KL}(P||q)} \geq 0 \quad (34)$$

since KL divergence is always non-negative. Thus,

$$\alpha > \frac{2 \text{KL}(q||P)}{\text{KL}(q||P) + \text{KL}(P||q)} \geq 0 \quad (35)$$

This implies there exists a positive value for α for any P and q such that $\widetilde{\mathcal{F}}_{JS-G}$ is greater than \mathcal{F}_{KL} .

Theorem 3. If P and q are Gaussian distributions with $P \sim \mathcal{N}(\mu_p, \sigma_p^2)$ and $q \sim \mathcal{N}(\mu_q, \sigma_q^2)$ then, $\exists \alpha \in [0, 1] : \widetilde{\mathcal{F}}_{JS-G} > \mathcal{F}_{KL}$ if and only if $\sigma_p^2 > \sigma_q^2$

Proof:

From Eq.(35) and $\alpha \in [0, 1]$ we have,

$$1 \geq \alpha > \frac{2 \text{KL}(q||P)}{\text{KL}(q||P) + \text{KL}(P||q)} > 0 \quad (36)$$

To satisfy inequality Eq.(36), we have the condition

$$1 > \frac{2 \text{KL}(q||P)}{\text{KL}(q||P) + \text{KL}(P||q)} \quad (37)$$

$$\implies \text{KL}(P||q) > \text{KL}(q||P) \quad (38)$$

Let, P and q be Gaussian distributions with $P \sim \mathcal{N}(\mu_p, \sigma_p^2)$ and $q \sim \mathcal{N}(\mu_q, \sigma_q^2)$. Then, Eq.(38) can be written as,

$$\ln \frac{\sigma_q^2}{\sigma_p^2} + \frac{\sigma_p^2 + (\mu_q - \mu_p)^2}{\sigma_q^2} - 1 > \ln \frac{\sigma_p^2}{\sigma_q^2} + \frac{\sigma_q^2 + (\mu_p - \mu_q)^2}{\sigma_p^2} - 1 \quad (39)$$

$$\frac{\sigma_p^2}{\sigma_q^2} + \ln \frac{\sigma_q^2}{\sigma_p^2} + \frac{(\mu_q - \mu_p)^2}{\sigma_q^2} - \frac{\sigma_q^2}{\sigma_p^2} + \ln \frac{\sigma_p^2}{\sigma_q^2} + \frac{(\mu_p - \mu_q)^2}{\sigma_p^2} > 0 \quad (40)$$

Let, $\gamma = \frac{\sigma_p^2}{\sigma_q^2}$. Eq.(40) can be rewritten as,

$$\gamma - \frac{1}{\gamma} + \ln \frac{1}{\gamma} - \ln \gamma + \frac{(\mu_q - \mu_p)^2}{\sigma_q^2} - \frac{(\mu_p - \mu_q)^2}{\gamma \sigma_q^2} > 0 \quad (41)$$

$$\gamma - \frac{1}{\gamma} + \ln \frac{1}{\gamma^2} + \frac{(\mu_q - \mu_p)^2}{\sigma_q^2} \left(1 - \frac{1}{\gamma}\right) > 0 \quad (42)$$

This condition Eq.(42) is satisfied when $\gamma > 1$ or

$$\sigma_p^2 > \sigma_q^2 \quad (43)$$

Thus, when P and q are Gaussian distributions with $\sigma_p^2 > \sigma_q^2$, there always exists an $\alpha \in [0, 1]$ such that $\widetilde{\mathcal{F}}_{JS-G} > \mathcal{F}_{KL}$. Therefore, Theorems 1 and 2 provide us with the conditions under which the JS-G divergence-based loss function regularises better than the KL divergence-based loss function.

2.7.3. Regularisation performance of JS-A divergence

Monte Carlo estimates of the KL divergence and the JS-A divergence for the distributions $q \sim \mathcal{N}(\mu_1 = \mu, \sigma_1^2 = 0.01)$ and $P \sim \mathcal{N}(\mu_2 = 0, \sigma_2^2 = 0.1)$ is presented in Fig.2. The JS-A divergence has a lesser value as compared to the KL divergence without considering the λ parameter. Nevertheless, by appropriately selecting the value of λ a higher value is obtained for the divergence as shown in Fig.2. Thus, the JS-A-based loss function $\widetilde{\mathcal{F}}_{JS-A}$ should result in better regularisation than the KL divergence-based loss function with appropriate hyperparameter values.

2.7.4. Monte Carlo estimates

A closed-form solution does not exist for KL and JS divergences for most combinations of prior and posterior distributions. In cases where such a closed form for the divergence is unavailable for a given distribution, we can resort to Monte Carlo (MC) estimates. However, the estimation of the loss function using MC estimates is computationally expensive. In addition, for networks with a large number of parameters, the memory requirement increases significantly with MC estimates. To estimate the number of MC samples required to achieve the accuracy of closed

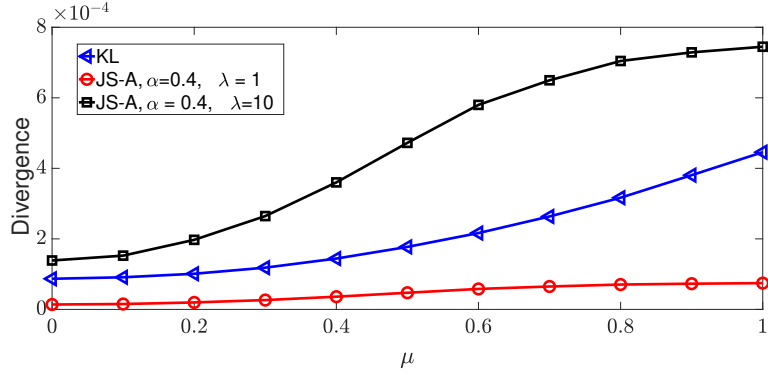


Figure 2: The value of KL and JS-A divergence evaluated using the MC approximation is plotted against the mean μ of q .

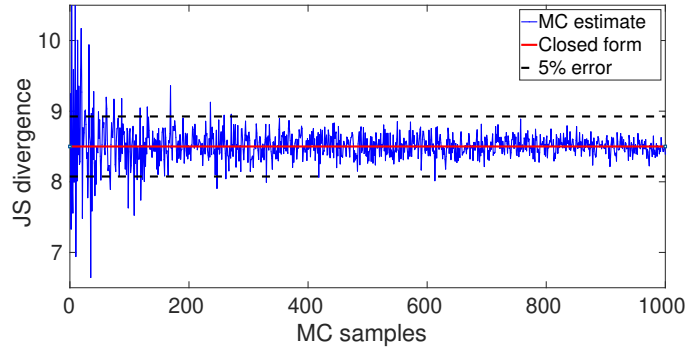


Figure 3: Comparison of MC estimates and the closed form solution of JS-G divergence demonstrating the benefit of closed form solution.

form estimates, JS-G divergence of two Gaussian distributions $\mathcal{N}(5, 1)$ and $\mathcal{N}(0, 1)$ are evaluated and compared with its closed form counterpart. Fig. 3 shows the results of the comparison. It is seen that at least 600 samples are required to estimate the JS-G divergence within 5% error. This implies evaluating the loss function 600 times for a given input and back-propagating the error which requires huge computational efforts. Therefore, utilizing the closed-form solution when available can save huge computational efforts and memory.

3. Experiments

To implement the proposed loss functions and demonstrate their advantages, we performed experiments and compared them with the existing ELBO loss Eq. (13). The details of the experiments are described in this section. We have used a closed-form implementation as proposed in algorithm 1 for the JS-G-based loss function and the Monte-Carlo implementation as proposed in algorithm 2 for the JS-A-based loss function in the experiments.

3.1. Data sets

Two Data sets were used to perform the experiments namely the CIFAR-10 data set and a publicly available histopathology data set.

3.1.1. CIFAR-10 data set

CIFAR-10 data set consists of 60,000 images of size $32 \times 32 \times 3$ belonging to 10 mutually exclusive classes. This dataset is an unbiased dataset with each of the 10 classes having 6,000 images. Images were normalized using the min-max normalization technique. To demonstrate the effectiveness of regularisation, varying levels of Gaussian

noise were added to the normalized CIFAR-10 data set. The entire dataset was split into 60%-20%-20% for training-validation-testing respectively. Three Bayesian CNNs with the same architecture were trained by: 1) minimizing the ELBO loss Eq. (13), 2) minimizing the proposed JS-G-based loss function $\tilde{\mathcal{F}}_{JSG}$ in Eq. (28) and 3) minimizing the proposed JS-A-based loss function $\tilde{\mathcal{F}}_{JSA}$ in Eq.(30).

3.1.2. Histopathology data set

To demonstrate the effectiveness of the loss function on a biased data set, we used a publicly available breast histopathology data set [30]. These are images containing regions of Invasive Ductal Carcinoma. The original data set consisted of 162 whole-mount slide images of Breast Cancer specimens scanned at 40x. From the original whole slide images, 277,524 patches of size $50 \times 50 \times 3$ pixels were extracted (198,738 negatives and 78,786 positives), labeled by pathologists, and provided as a data set for classification.

The data set consists of two classes: positive (1) and negative (0). 20% of the entire data set was used as the testing set for our study. The remaining 80% of the entire data was further split into a training set and a validation set (80%-20% split) to perform hyperparameter optimization. The images were shuffled and converted from uint8 to float format for normalizing. As a post-processing step, we computed the complement of all the images (training and testing) and then used them as inputs to the neural network. The pixel-wise normalization and complement were carried out as $p_n = (255 - p)/255$. Where p is the original pixel value and p_n is the pixel value after normalization and complement.

3.2. Hyperparameter optimisation and network Architecture

Hyperparameters for all the networks considered here are chosen through hyperparameter optimization. A Tree-structured Parzen Estimator (TPE) algorithm, which is a sequential model-based optimization approach, is used [31]. In this approach, models are constructed to approximate the performance of hyperparameters based on historical measurements. New hyperparameters are chosen based on this model to evaluate performance. A python library Hyperopt [32] is used to implement this optimization algorithm over a given search space. Data is split into a training set and a validation set as explained in section 3.1. An optimization is performed to maximize the validation accuracy for different hyperparameter settings of the network.

The architecture of all the networks used in this work follows the ResNet-18 V1 model [33] without the batch normalization layers. The network parameters are initialized with the weights of ResNet-18 trained on the Imagenet data set[34]

4. Results and discussions

This section presents the classification results on the noisy CIFAR and the biased histopathology data sets. A comparison of the performance is presented between the existing KL divergence-based loss function and the JS divergence-based loss functions proposed in this work.

4.1. Results of hyperparameter optimization

Results of the hyperparameter optimization (described in Section. 3.2) for the two data sets are presented in Tables. 2 and 3. In Table. 2 LR is the learning rate. λ is taken as 1 for the JS-G divergence-based loss function throughout this work.

4.2. Training and Validation

The data set was split into a training, a validation, and a test set as explained in Section. 3.1. Training of the networks is done until the loss converges or the validation accuracy starts to decrease. The test results provided in the upcoming sections correspond to the epoch in which the validation accuracy was maximum.

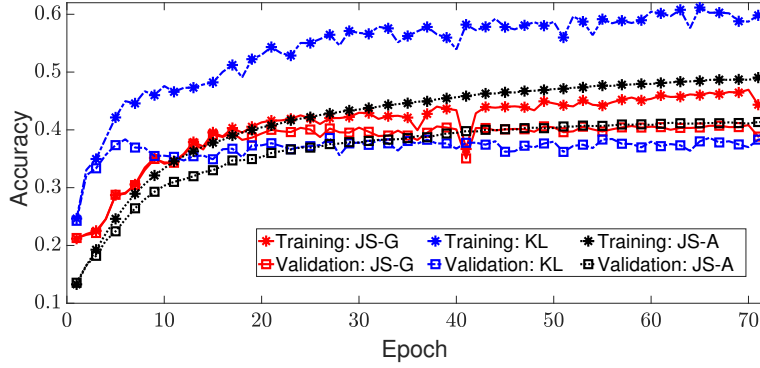
Table 2: CIFAR10 dataset

Divergence	Parameter	Noise level (σ)				
		0.1	0.2	0.3	0.4	0.5
KL	LR	1e-4	1e-4	1e-4	1e-3	1e-3
JS-G	α	0.004	0.1313	0.2855	0.3052	0.2637
	LR	1e-4	1e-4	1e-4	1e-4	1e-5
JS-A	λ	1000	1000	1000	1000	1000
	α	0.7584	0.6324	0.1381	0.6286	0.1588
	LR	1e-4	1e-4	1e-4	1e-3	1e-4

Divergence	Parameter	Noise level (σ)			
		0.6	0.7	0.8	0.9
KL	LR	1e-3	1e-3	1e-3	1e-3
JS-G	α	0.2249	0.3704	0.3893	0.7584
	LR	1e-4	1e-4	1e-5	1e-3
JS-A	λ	100	1000	1e4	1e5
	α	0.4630	0.1220	0.2282	0.5792
	LR	1e-3	1e-4	1e-5	1e-5

Table 3: Histopathology dataset

Divergence	α	λ	Learning rate
JS-G	0.0838	1	1e-4
JS-A	0.0729	100	1e-4
KL	-	-	1e-4

Figure 4: Training and validation of CIFAR 10 dataset with added Gaussian noise $\mathcal{N}(\mu = 0, \sigma = 0.9)$ using the KL-loss function and the proposed JS divergence-based loss functions.

4.2.1. CIFAR 10

Training of the CIFAR 10 dataset is performed with varying levels of noise intensity. Accuracy of training and validation sets for noise $\mathcal{N}(\mu = 0, \sigma = 0.9)$ is presented for both KL divergence-based loss function and the proposed JS divergence-based loss functions in Fig. 4. It is observed from Fig. 4 that KL divergence-based loss function over-fits the training data by learning the noise whereas the JS divergence-based loss functions regularise better showing better generalization for the unseen validation dataset. The JS divergence-based loss function also provides better results in terms of accuracy in classifying validation and test sets. Although a representative case of $\sigma = 0.9$ is presented here, a similar trend was observed for other noise levels as well.

4.2.2. Histopathology

Training of the histopathology dataset is performed using the hyperparameters obtained in Table. 3. A learning rate scheduler is used during training in which the learning rate is multiplied by a factor of 0.1 in the 4th, 8th, 12th, and 20th epochs. Fig. 5 shows the accuracy of training and validation sets for the KL divergence-based loss function and the proposed JS divergence-based loss function. Similar to the noisy CIFAR-10 data set, the KL divergence-based loss

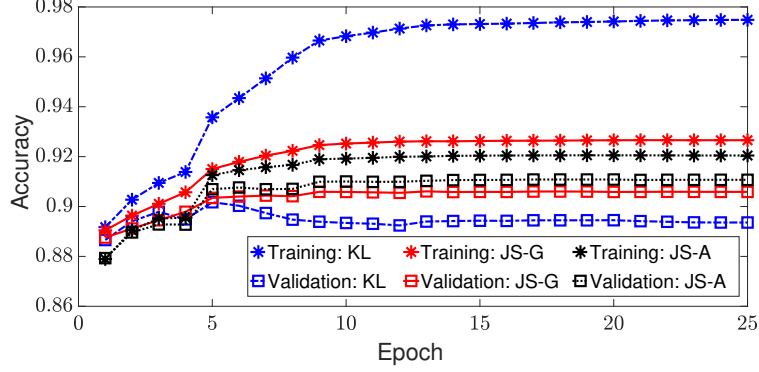


Figure 5: Training and validation of histopathology dataset using the KL-loss function and the proposed JS divergence-based loss functions.

function learns the training data too well and fails to generalize for the unseen validation set. Whereas, the proposed JS divergence-based loss functions regularise better and provide more accurate results for the validation and test sets.

4.3. Testing

Results obtained on the test sets of noisy CIFAR-10 data sets and the histopathology data set are presented in this section. Five runs were performed with different mutually exclusive training and validation tests to compare the results of the KL divergence-based loss function and the proposed JS divergence-based loss functions.

4.3.1. CIFAR 10

The accuracy of the noisy CIFAR 10 test data set at varying noise levels is presented in Fig. 6 and Fig. 7. It is

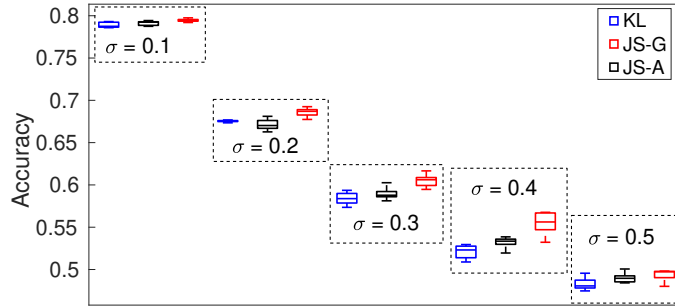


Figure 6: Accuracy on the test data set at different noise levels (from $\sigma = 0.1$ to $\sigma = 0.5$). Each box chart displays the median as the center line, the lower and upper quartiles as the box edges, and the minimum and maximum values as whiskers.

observed from Fig. 6 and Fig. 7 that the accuracy of both the proposed JS divergence-based loss functions is better in all the noise level cases. It is also seen that the difference in accuracy between KL divergence-based loss and the JS divergence-based losses increases with increasing noise levels. This demonstrates the regularising capability of the proposed JS divergence-based loss functions.

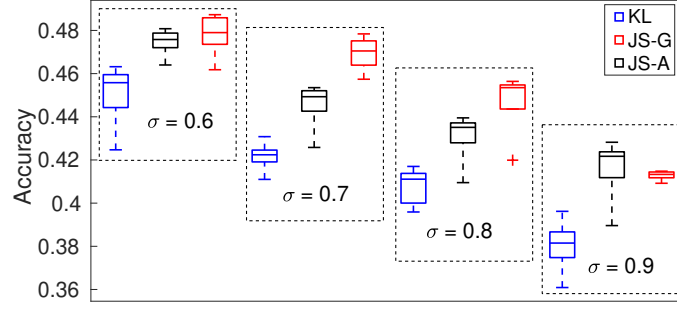


Figure 7: Accuracy on the test data set at different noise levels (from $\sigma = 0.6$ to $\sigma = 0.9$). Each box chart displays the median as the center line, the lower and upper quartiles as the box edges, and the minimum and maximum values as whiskers.

4.3.2. Histopathology

The results of the five runs of the KL divergence-based loss function and the proposed JS divergence-based loss functions on the biased histopathology data set are presented in this section.

It is evident from Fig. 8 that both the proposed JS divergence-based loss functions perform better than the existing

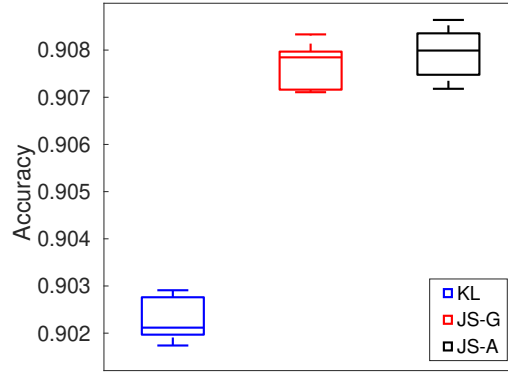


Figure 8: Accuracy on the test data set for five runs. Each box chart displays the median as the center line, the lower and upper quartiles as the box edges, and the minimum and maximum values as whiskers.

KL divergence-based loss function in all five runs with different training and validation sets. Since this data set is biased toward the negative class, the improvement in performance shown by the proposed JS divergence-based loss functions is attributed to better regularisation and generalization capabilities of the loss functions. The receiver

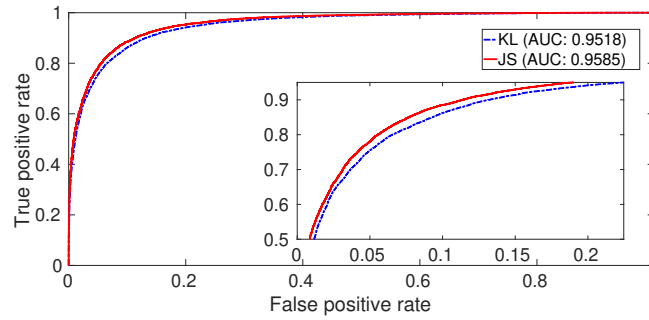


Figure 9: Receiver operating characteristic curve depicting the classification performance of the three binary classifiers studied.

operating characteristic (ROC) curve is a performance evaluation metric that visually plots the classification ability of a binary classifier when the discrimination threshold is varied. For this binary classification problem on histopathology data set the ROC curve is plotted in Fig. 9. It is seen from the values of the area under the curve (AUC) that both the proposed JS divergence-based loss functions perform better than the existing KL divergence-based loss function. Confusion matrices for the proposed JS divergence-based loss function and the existing KL divergence-based loss

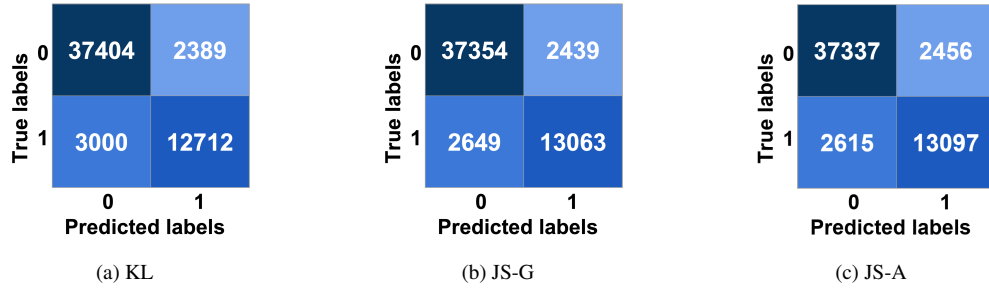


Figure 10: Confusion matrices for (a) KL divergence-based loss function and (b) Skew-geometric JS divergence-based loss function (c) Modified generalized JS divergence on the histopathology data set.

function are shown in Fig.10. It is observed from Fig. 10 that in addition to improving the accuracy of predictions, the proposed JS-G divergence-based loss function and the JS-A divergence-based loss function reduce the number of false negative predictions by 11.7% and 12.8% respectively, as compared to the existing KL divergence-based loss function. Given that the data set is biased towards the negative class, this is a significant achievement.

5. Conclusions

In this study, we introduced two novel JS divergence-based loss functions for Bayesian neural networks that extend the state-of-the-art loss function. The proposed loss functions generalize well for noisy and biased data sets. To conclude this study, we summarise its main findings as follows.

Firstly, we have formulated two JS Divergence based loss functions for Bayesian neural networks and have shown that these are a generalization of the widely used KL divergence-based loss function.

Secondly, we have explained the reason why the proposed loss functions will perform better than the state-of-the-art. Further, we have derived the conditions to obtain better regularisation through the proposed JS-G divergence-based loss function for Gaussian priors and posteriors.

Thirdly, we have provided algorithms for the closed-form evaluation as well as the Monte Carlo approximation of the proposed loss functions. The relative merits of these two approaches are discussed.

Fourthly, we have shown the improvement in performance achieved by the proposed loss functions in terms of various performance metrics on data sets having bias and various degrees of noise.

This work would serve as a foundation for exploring other divergences for variational inferences in machine learning models.

References

- [1] G. Litjens, T. Kooi, B. E. Bejnordi, A. A. A. Setio, F. Ciompi, M. Ghafoorian, J. A. Van Der Laak, B. Van Ginneken, and C. I. Sánchez, "A survey on deep learning in medical image analysis," *Medical image analysis*, vol. 42, pp. 60–88, 2017.
- [2] D. Shen, G. Wu, and H.-I. Suk, "Deep learning in medical image analysis," *Annual review of biomedical engineering*, vol. 19, p. 221, 2017.
- [3] P. Thiagarajan, P. Khairnar, and S. Ghosh, "Explanation and use of uncertainty quantified by bayesian neural network classifiers for breast histopathology images," *IEEE Transactions on Medical Imaging*, vol. 41, no. 4, pp. 815–825, 2021.
- [4] M. Frank, D. Drikakis, and V. Charissis, "Machine-learning methods for computational science and engineering," *Computation*, vol. 8, no. 1, p. 15, 2020.
- [5] S. Kollmannsberger, D. D'Angella, M. Jokeit, L. Herrmann, *et al.*, *Deep Learning in Computational Mechanics*. Springer, 2021.
- [6] U. Yadav, S. Pathrudkar, and S. Ghosh, "Interpretable machine learning model for the deformation of multiwalled carbon nanotubes," *Physical Review B*, vol. 103, no. 3, p. 035407, 2021.

- [7] K. Choudhary, B. DeCost, C. Chen, A. Jain, F. Tavazza, R. Cohn, C. W. Park, A. Choudhary, A. Agrawal, S. J. Billinge, *et al.*, “Recent advances and applications of deep learning methods in materials science,” *npj Computational Materials*, vol. 8, no. 1, pp. 1–26, 2022.
- [8] S. Pathrudkar, H. M. Yu, S. Ghosh, and A. S. Banerjee, “Machine learning based prediction of the electronic structure of quasi-one-dimensional materials under strain,” *Physical Review B*, vol. 105, no. 19, p. 195141, 2022.
- [9] C. Beck, M. Hutzenhaler, A. Jentzen, and B. Kuckuck, “An overview on deep learning-based approximation methods for partial differential equations,” *arXiv preprint arXiv:2012.12348*, 2020.
- [10] R. Matthey and S. Ghosh, “A novel sequential method to train physics informed neural networks for allen cahn and cahn hilliard equations,” *Computer Methods in Applied Mechanics and Engineering*, vol. 390, p. 114474, 2022.
- [11] M. Buda, A. Maki, and M. A. Mazurowski, “A systematic study of the class imbalance problem in convolutional neural networks,” *Neural Networks*, vol. 106, pp. 249–259, 2018.
- [12] H. D. Kabir, A. Khosravi, M. A. Hosen, and S. Nahavandi, “Neural network-based uncertainty quantification: A survey of methodologies and applications,” *IEEE access*, vol. 6, pp. 36218–36234, 2018.
- [13] L. V. Jospin, H. Laga, F. Boussaid, W. Buntine, and M. Bennamoun, “Hands-on bayesian neural networks—a tutorial for deep learning users,” *IEEE Computational Intelligence Magazine*, vol. 17, no. 2, pp. 29–48, 2022.
- [14] N. Tishby, E. Levin, and S. A. Solla, “Consistent inference of probabilities in layered networks: Predictions and generalization,” in *International Joint Conference on Neural Networks*, vol. 2, pp. 403–409, IEEE New York, 1989.
- [15] J. Denker and Y. LeCun, “Transforming neural-net output levels to probability distributions,” *Advances in neural information processing systems*, vol. 3, 1990.
- [16] E. Goan and C. Fookes, *Bayesian Neural Networks: An Introduction and Survey*, pp. 45–87. Cham: Springer International Publishing, 2020.
- [17] Y. Gal, “Uncertainty in deep learning,” *PhD thesis, University of Cambridge*, 2016.
- [18] C. P. Robert, V. Elvira, N. Tawn, and C. Wu, “Accelerating mcmc algorithms,” *Wiley Interdisciplinary Reviews: Computational Statistics*, vol. 10, no. 5, p. e1435, 2018.
- [19] G. E. Hinton and D. Van Camp, “Keeping the neural networks simple by minimizing the description length of the weights,” in *Proceedings of the sixth annual conference on Computational learning theory*, pp. 5–13, 1993.
- [20] D. Barber and C. M. Bishop, “Ensemble learning in bayesian neural networks,” *Nato ASI Series F Computer and Systems Sciences*, vol. 168, pp. 215–238, 1998.
- [21] A. Graves, “Practical variational inference for neural networks,” *Advances in neural information processing systems*, vol. 24, 2011.
- [22] J. M. Hernández-Lobato and R. Adams, “Probabilistic backpropagation for scalable learning of bayesian neural networks,” in *International conference on machine learning*, pp. 1861–1869, Proceedings of Machine Learning Research, 2015.
- [23] C. Blundell, J. Cornebise, K. Kavukcuoglu, and D. Wierstra, “Weight uncertainty in neural network,” in *International conference on machine learning*, pp. 1613–1622, Proceedings of Machine Learning Research, 2015.
- [24] J. Hensman, M. Zwiëbele, and N. D. Lawrence, “Tilted variational bayes,” in *Artificial Intelligence and Statistics*, pp. 356–364, Proceedings of Machine Learning Research, 2014.
- [25] Y. Li and R. E. Turner, “Rényi divergence variational inference,” *Advances in neural information processing systems*, vol. 29, 2016.
- [26] A. B. Dieng, D. Tran, R. Ranganath, J. Paisley, and D. Blei, “Variational inference via χ upper bound minimization,” *Advances in Neural Information Processing Systems*, vol. 30, 2017.
- [27] J. Deasy, N. Simidjevski, and P. Liò, “Constraining variational inference with geometric jensen-shannon divergence,” *Advances in Neural Information Processing Systems*, vol. 33, pp. 10647–10658, 2020.
- [28] F. Nielsen, “On the jensen–shannon symmetrization of distances relying on abstract means,” *Entropy*, vol. 21, no. 5, p. 485, 2019.
- [29] I. Higgins, L. Matthey, A. Pal, C. Burgess, X. Glorot, M. Botvinick, S. Mohamed, and A. Lerchner, “beta-VAE: Learning basic visual concepts with a constrained variational framework,” in *International Conference on Learning Representations*, 2017.
- [30] Paul Mooney, “Breast Histopathology Images.” <https://www.kaggle.com/paultimothymooney/breast-histopathology-images>. 2017.
- [31] J. Bergstra, R. Bardenet, Y. Bengio, and B. Kégl, “Algorithms for hyper-parameter optimization,” in *25th annual conference on neural information processing systems (NIPS 2011)*, vol. 24, Neural Information Processing Systems Foundation, 2011.
- [32] J. Bergstra, D. Yamins, and D. Cox, “Making a science of model search: Hyperparameter optimization in hundreds of dimensions for vision architectures,” in *International conference on machine learning*, pp. 115–123, Proceedings of Machine Learning Research, 2013.
- [33] K. He, X. Zhang, S. Ren, and J. Sun, “Deep residual learning for image recognition,” in *Proceedings of the IEEE conference on computer vision and pattern recognition*, pp. 770–778, 2016.
- [34] A. Krizhevsky, I. Sutskever, and G. E. Hinton, “Imagenet classification with deep convolutional neural networks,” in *Advances in neural information processing systems*, pp. 1097–1105, 2012.